Journal of Applied Research in Science and Humanities

Study of microstructure development and mechanical characteristics of tin–antimony and tin–antimony–silver lead free solder alloys for microelectronic applications

Reem Hesham Abdel Wahab, **Sarah Ashraf Rashad**, **Sarah Hamdy Abdelkhelik**, **Sarah Moheb Nassif**, **Salma Ahmed Hasan**, **Salma Ahmed AbdelFattah**, **Salma Samir Mohamed**.

Supervisor: **Dr**. **Maha Mahmoud Mousa**, **lecturer**, **solid state physics**

Ain Shams University, **Faculty of Education**, **Bachelor's program in Science and Education** (**primary**), **Science–Private**.

Abstract

This study examined the effects of incorporating 1 weight percent Ag element into Sn–5wt%Sb lead free solder on the microstructure and tensile stress strain properties. Optical microscopy (OM), scanning electron microscopy (SEM) and energy dispersive X-ray spectroscopy (EDS) were used to analyse the microstructure of both alloys. In addition to forming Ag_3Sn IMC with uniform distribution, microstructural investigations showed that adding Ag element to Sn–5wt%Sb solder results in the β-Sn phase's grain refinement. The tensile measurements were carried out at testing temperatures of 25 and 60 °C at a variety of strain rates ($\dot{\varepsilon}$), from 2.05×10^{-4} to 1×10^{-3} sec^{-1}. According to the experimental data, the yield stress (σ_Y) and ultimate tensile strength (σ_{UTS}) of the materials under study rise with the addition of Ag and an increase in the strain rates ($\dot{\varepsilon}$), whereas they decrease with an increase in the deformation temperature. All of the solder alloys that were evaluated had stress exponent values between 2.82 and 6.73.

Key Words:

Sn-Sb; Ag addition; Microstructure; Stress–strain curves

1. **Introduction**:

In the latter half of the 20th century, increased awareness of lead toxicity fuelled the switch from lead-based to lead-free solder alloys, ultimately resulting in legislative measures like the 2006 Restriction of Hazardous Substances (RoHS) directive from the European Union [M. Abtew 2000]. The industry standard in the past was tin-lead (Sn-Pb) alloys because of its superior mechanical qualities, low melting points, and simplicity of use. But worries about the negative effects of lead exposure on the environment and human health have made the switch to lead-free alternatives necessary. Lead is a known toxic material. Serious health issues, including as brain damage and developmental delays in children, can result from even very little exposure. Furthermore, because lead seeps into soil and water sources, inappropriate disposal of lead-based items exacerbates environmental contamination. In response to these risks, regulatory agencies such as the European Union adopted the RoHS directive in 2006, which prohibits the use of lead in electrical and electronic devices. The development and broad use of lead-free solder alloys have been fuelled by this regulation [E.A. Eid 2019].

Lead-free solder alloys have many different and wide-ranging uses. They are important to produce consumer electronics, from computers to cell phones, providing dependable operation and adherence to environmental requirements. Lead-free solders are essential in the automobile industry for producing sensors, electronic control units, and other parts that must withstand hard operating conditions. Aerospace sectors need solders with outstanding toughness and resistance to thermal cycling, making tin-antimony-silver alloys an appropriate choice. Also, these materials are essential to renewable energy technologies where environmental sustainability and durability are top concerns, such wind turbines and solar panels [Edmond Chan, 2004].

As a replacement for lead-based solder, various alternative alloys have been developed, including tin-antimony (Sn-Sb) solder alloys being among the most widely used. Tin-antimony solders are a dependable connector material for semiconductor devices, providing perfect thermal and electrical performance. They are also used in aerospace applications, where high dependability and its long life are required. Sn-Sb alloys are widely used because of a number of benefits, including as their excellent mechanical strength and low melting point, which reduces thermal stress on delicate electronic components during soldering. making them appropriate for uses where strong, long-lasting joints are needed. Additionally, Sn-Sb alloys are an environmentally favorable substitute for conventional lead-based solders because they are lead-free and adhere to environmental requirements [Morozumi 2015].

Understanding phase diagrams for alloy systems is essential because mechanical properties and microstructure have a close connection, and an

alloy's microstructure development is influenced by the features of its phase diagram. Also, phase diagrams give important details regarding melting, casting, crystallization, and other processes [OH, 2004]. The eutectic point, or the lowest temperature at which an individual combination of substances may stay in the liquid phase, is an important aspect of phase diagrams. As it determines the solidification behaviour and mechanical characteristics of materials, understanding this point is essential for alloy design. Eutectic Point: Has a melting point of around 243°C and occurs at 97.5% tin (Sn) and 2.5% antimony (Sb). Because of the alloy's high melting point, soldering benefits from the direct transition from liquid to solid at this composition [Zu et al , 2006].

Kyosuke Kobayashi (2017) investigated the fracture behaviors of Sn-5Sb solder specimens under fatigue and tensile forces. The results indicate that tensile strength increase with strain rate but drop as temperature rises. It may be possible to inhibit grain boundary sliding, decrease grain development, and increase solder junction reliability by adding ternary or quaternary additions to Sn-5Sb. M. M.Mousa (2024) investigated how the presence of Cr affected the tensile characteristics and microstructural changes of Sn-5 weight percent Sb solder . This study is interesting since it is the first to link the microstructure of Sn-5wt% Sb solder alloy reinforced with varying Cr concentrations to its tensile characteristics. Silver improves wettability and reduces the formation of brittle intermetallic compounds, resulting in strong and reliable joints in microelectronic devices. These alloys outperform traditional lead-based solders in demanding applications due to their higher safety profile and environmental sustainability [Y. Swilem 2009]. Tianhan Hu (2023) compared the mechanical characteristics and microstructure of Sn–Bi solder alloys with different additions of silver and indium. According to the findings, the solder alloy's tensile strength and ductility might be significantly increased. The microstructure is much improved by the inclusion of Ag and In. In the Sn matrix, element In solutes, whereas element Ag prefers to form the Ag3Sn phase. The current study aims to examine the development of microstructures and mechanical characteristics of Sn- 5 wt.% Sb and Sn- 5 wt.% Sb-1Ag wt.% solder alloys.

2.Methods of Research and the tools used

The present research examined two different types of solders: Sn-5 wt.% Sb and Sn-5 wt.% Sb-1 wt.% Ag. Superior purity tin (Sn), antimony (Sb), and silver (Ag) (99.99%) were used as raw materials to create the two alloys. A vacuum furnace was used to melt the Sn for two hours at 650 degrees Celsius in order to completely dissolve it. The molten alloys were chilled and poured into stainless steel molds at room temperature. Swinging and cold drawing

were used to create (i) 1 mm thick discs for microstructure inspection and (ii) wire samples with a 0.9 mm diameter and 30 mm length for tensile testing from the alloys under investigation.

For metallographic analysis, the disc pieces had been etched in a 95 volume percent ethyl alcohol and 5 volume percent nitric acid solution. OM and FE-SEM equipped with EDX were used to analyze the microstructures of the alloys. The optical microscope is connected to a PC have a digital-image-analysis software.

Stress-strain measurements are carried out at various testing temperatures (25, 60 °C) utilizing a computerized tensile testing apparatus. Four different strain rates (2.05×10^{-4}, 4.67×10^{-4}, 7.51×10^{-4}, and 1×10^{-3} ses^{-1}) were used at each test temperature. Tensile testing was carried out on wire specimens that were 0.9 mm in diameter and 30 mm in length until they fractured. The sample was stretched by the motor in one direction. The rotational motion sensor simultaneously measures the sample's strain while the force sensor records the applied force during stretching. Stress and strain can be computed and a stress-strain curve can be created using a data studio software program installed on a PC computer to identify the signal originating from the interface that was gathered from the force and rotating motion sensors.

3. Results and Discussion of Research

3.1 Microstructure investigations

Figure 1 illustrates the Sn-rich portion of the phase diagram for Sn-Sb [T. Kobayashi, 20018]. This diagram demonstrates that the Sn-5Sb alloy's microstructure is made up of SbSn IMC and β-Sn phase. According to Chen [S.W. Chen, 2008], the Sn_3Sb_2 phase developed throughout the solidification process. Below 242 °C, it breaks down into the β-Sn and the SbSn IMC. Figure 2 (a,b) show OM micrographs of Sn-5Sb and Sn-5Sb-1Ag alloys respectively. while figure 3 (a,b) show OM micrographs with high magnifications. These figures demonstrate the microstructure of the Sn–5Sb alloy is made up of β-Sn and a dispersion of SbSn phase along the grain boundaries as round, white particles.

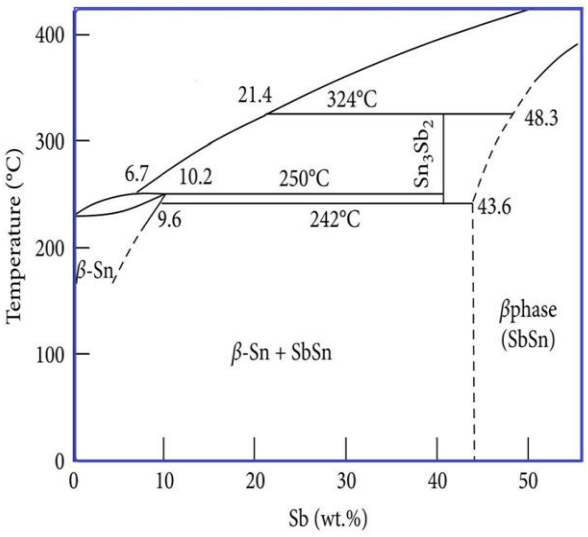

Figure 1: phase diagram of the Sn-Sb [T. Kobayashi, 20018].

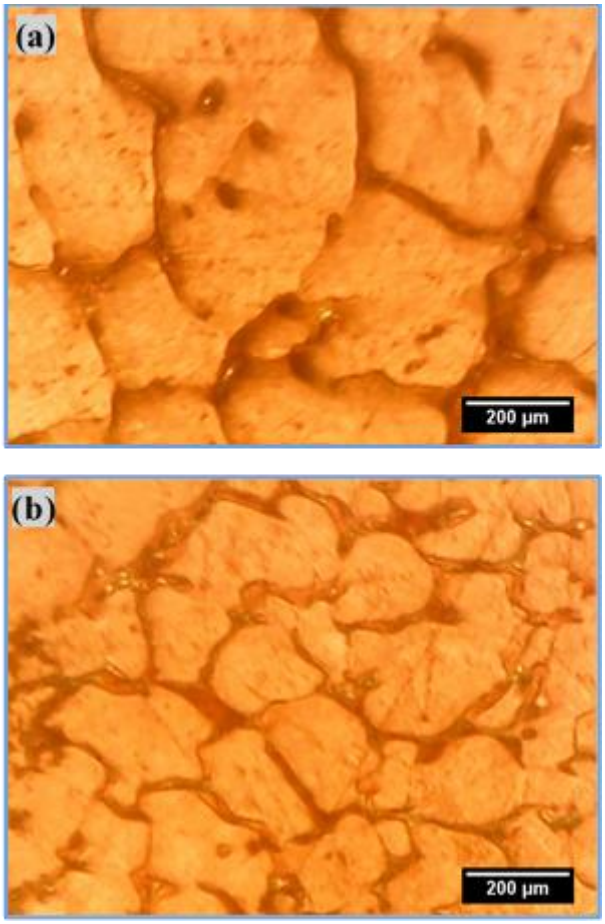

Figure 2: OM micrographs of (a) Sn-5Sb and (b) Sn-5Sb-1Ag alloys

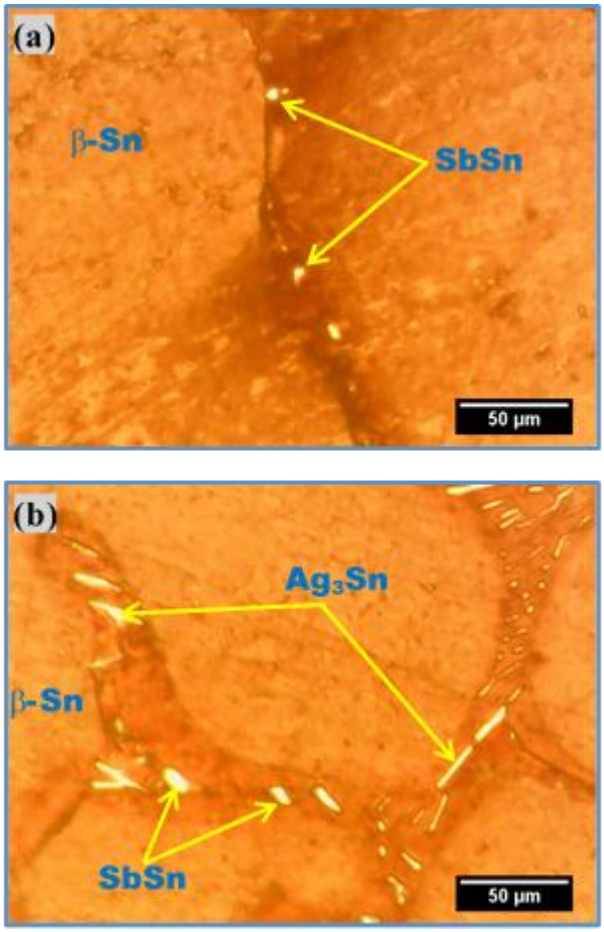

Figure 3: High magnification of OM micrographs of (a) Sn-5Sb and (b) Sn-5Sb-1Ag alloys

When 1 weight percent Ag was added to Sn-5Sb solder alloy, the grain size of the β-Sn matrix decreased, and a long rod-shaped Ag_3Sn intermetallic compound formed. Hence, the addition of Ag has a significant impact on grain size. One possible explanation for this action is that the Ag particles serve as pinning centers, reducing the dislocations' movement and promoting grain refining. This matches the findings of previous studies [A.R. Geranmayeh 2005, J.H. Kim 2002, A. Sadeghi 2024]

Field emission scanning electronic microscope pictures of Sn-5Sb-1Ag solder are shown in Figure 4. Long rod-shaped Ag_3Sn phase and a gray network of β-Sn grains with SbSn IMC (separated white spherical particles) are shown in the figure. The presence of Sn, Sb, and Ag components in the eutectic region of Sn-5Sb-1Ag alloy was verified by EDS analysis (see figure4).

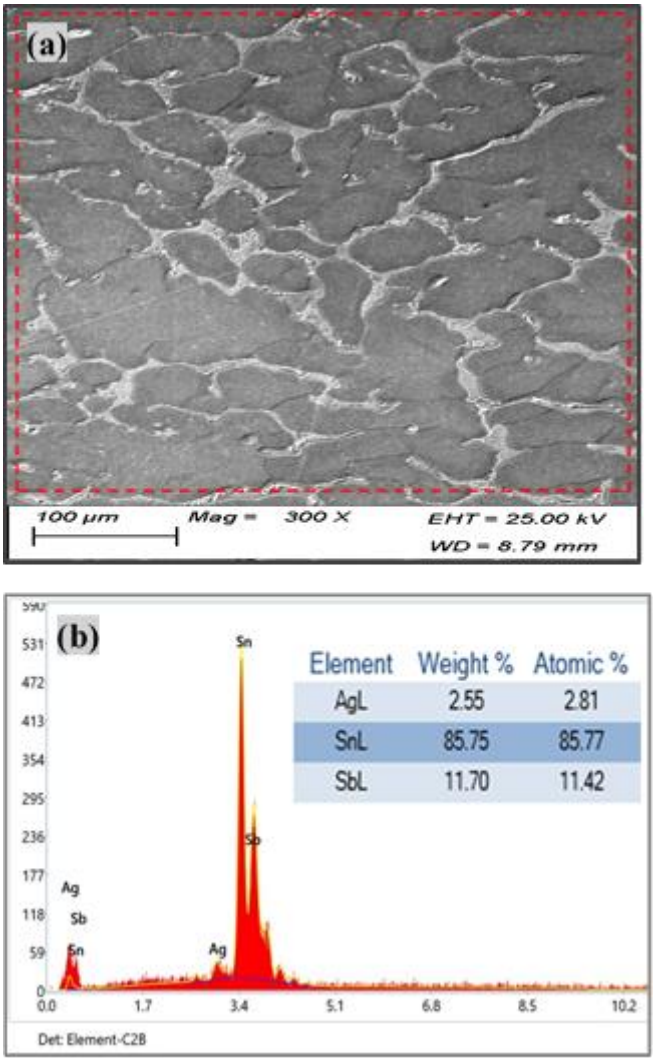

Figure 4: (a) SEM micrograph of Sn-5Sb-1Ag alloy and (b) corresponding EDX analysis.

3.2. Mechanical properties

The stress-strain characteristics of the Sn-5Sb and Sn-5Sb-1Ag alloys were examined with different strain rates ($\dot{\varepsilon}$) between 2.05×10^{-4} and 1×10^{-3} sec.$^{-1}$, and testing temperatures of 25 and 60 °C. The two alloys' stress-strain graphs at ambient temperature and at different strain rates of 2.05×10^{-4}, 4.67×10^{-4}, 7.51×10^{-4}, and 1×10-3 sec.$^{-1}$) are shown in Figure 5 (a,b). Figure 6 displays the stress-strain curves for two alloys at 60 oC and at earlier strain rates. These findings demonstrate that the stress-strain characteristics of samples are significantly impacted by variations in strain rate. For all alloys under study, higher values of ultimate tensile strength (σ_{UTS}) and yield stress (σ_Y) are obtained by increasing the strain rate when the temperature stays the same. This is because the number of dislocations rises in proportion to an increase in strain rate [A. Sadeghi, 2024].

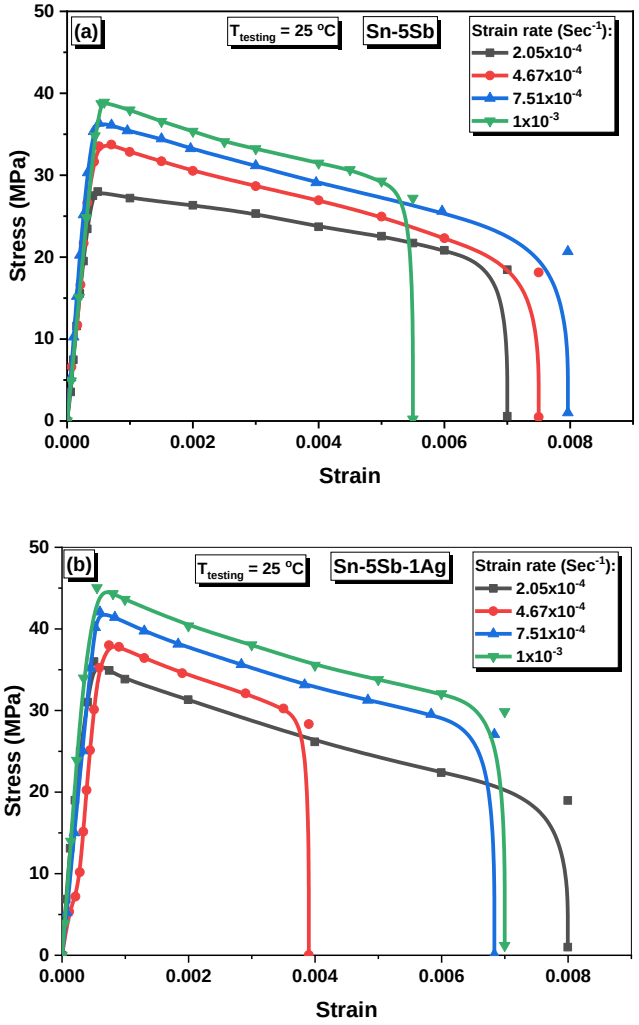

Figure 5: stress-strain curves of (a) Sn-5Sb and (b) Sn-5Sb-1Ag alloys at 25 °C with different strain rates

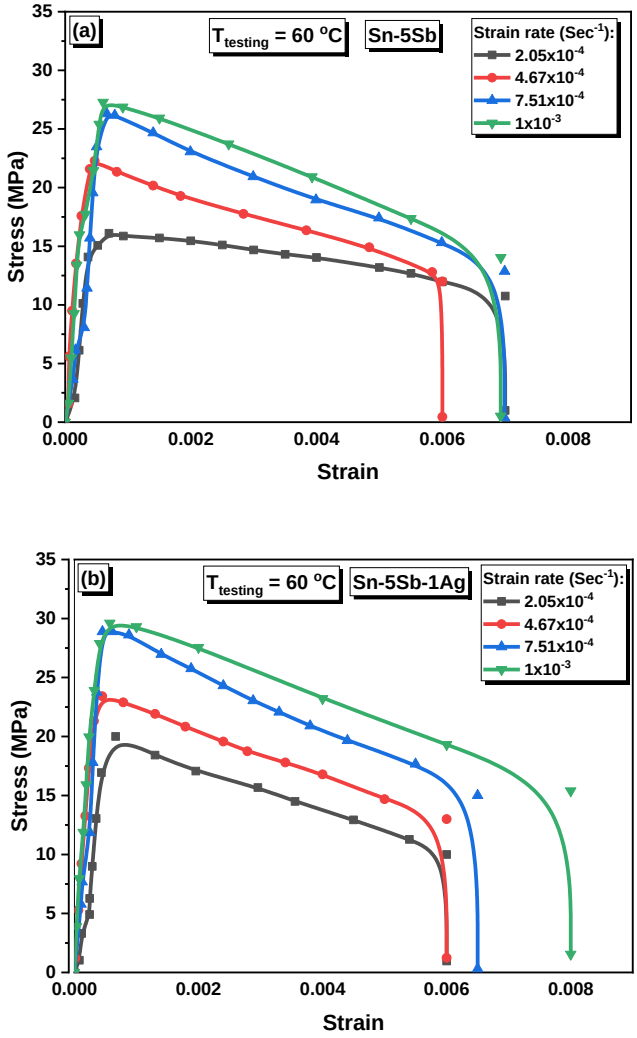

Figure 6: stress-strain curves of (a) Sn-5Sb and (b) Sn-5Sb-1Ag alloys at 60 °C with different strain rates.

At varying deformation temperatures and with the same strain rate of 1×10^{-3} sec^{-1}, Figure 7 displays representative stress-strain curves for the two alloys. From Tables 1 and 2, It is important to note that as deformation temperatures rise, σ_Y and σ_{UTS} monotonically move towards lower values. As the temperature rises, less hardening occurs because dislocation elimination occurs far more quickly than dislocation production [M.M. Mousa 2023].

However, i) the creation of a new Ag_3Sn phase and ii) a significant decrease in β-Sn grains are the primary causes of the observed strength increase with Ag addition.

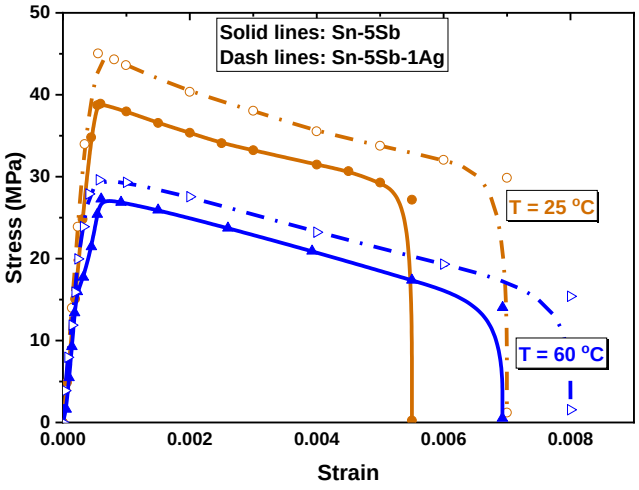

Figure 7: stress-strain curves of Sn-5Sb and Sn-5Sb-1Ag alloys at strain rate = $1x10^{-3}$ sec^{-1} with different temperatures.

Table 1: Values of σ_y for the studied alloys at different temperatures and strain rates.

Strain rate (Sec^{-1})	Yield stress (σ_y) (MPa)			
	Sn–5Sb		Sn–5Sb–1Ag	
	25 °C	60 °C	25 °C	60 °C
$2.05x10^{-4}$	27.44	14.49	35.02	17.81
$4.67x10^{-4}$	32.4	20.97	35.43	21.8
$7.51x10^{-4}$	35.3	24.62	41.28	27.71
$1x10^{-3}$	37.17	25.87	43.01	28.27

Table 2: Values of σ_{UTS} for the studied alloys at different temperatures and strain rates.

Strain rate (Sec^{-1})	Ultimate tensile strength (σ_{UTS}) (MPa)			
	Sn–5Sb		Sn–5Sb–1Ag	
	25 °C	60 °C	25 °C	60 °C
$2.05x10^{-4}$	28	16	36	20
$4.67x10^{-4}$	33.75	22.27	38	23.41
$7.51x10^{-4}$	36.35	26.3	42.07	28.88
$1x10^{-3}$	38.91	27.27	45.08	29.61

The relationship between the strain rate, $\dot{\varepsilon}$, σ_Y and σ_{UTS} for all samples at different temperatures is shown in Figures 8 and 9. It was previously reported that the ultimate tensile strength, σ_{UTS}, was significantly influenced by the strain rate, $\dot{\varepsilon}$. This dependence is expressed by the equation (1) [Q.S. Zhu, 2009]:

$$\dot{\varepsilon} = C\,\sigma_{UTS}^{n} \qquad (1)$$

where C is the material constant, and n is the stress exponent.

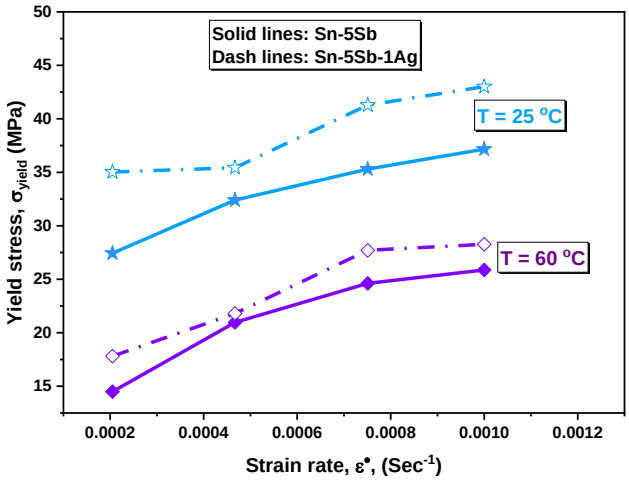

Figure 8: The relation between $\dot{\varepsilon}$ and σ_y for two samples at different temperatures

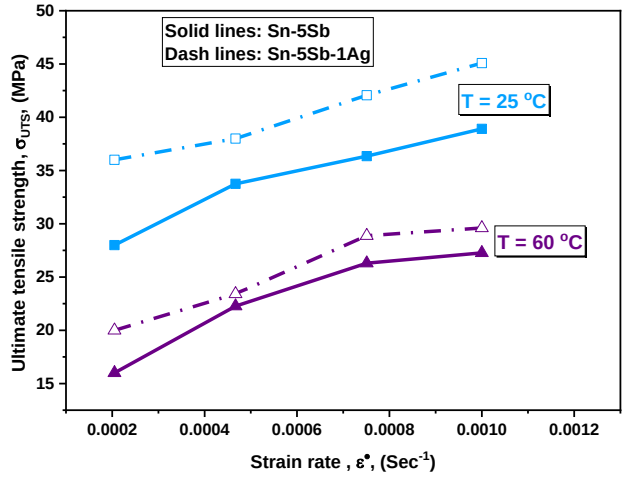

Figure 9: The relation between $\dot{\varepsilon}$ and σ_{UTS} for two samples at different temperatures.

Figure 10 shows a logarithmic plot of the ($\dot{\varepsilon}$) against the σ_{UTS} for both alloys at various deformation temperatures. The slope of straight line obtained from this figure is equal to the stress exponent. Figure 11 displays the relationship

between n and temperature of alloys under investigation. The values of n clearly decrease with increasing deformation temperature, but increase with increasing Ag concentration.

In the current research, the values of n of Sn-5Sb are 4.87 and 2.82 at 25 and 60 respectively. while the values of n of Sn-5Sb-1Ag range from 6.87 to 3.66 at the same testing temperature, as shown in Figure 11. This result's interpretation is predicated on the fact that n denotes the alloy's capacity for necking resistance or its ability to elongate without rupturing. [K.C. Cham 2001]. As a result, it was observed that the Ag-containing alloy had greater resistance to necking.

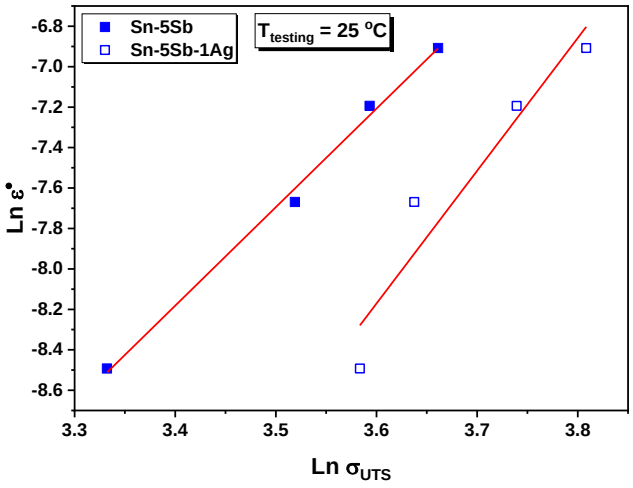

Figure 9: The relation between ln σ_{UTS} and ln ε• for two samples at temperatures 25 °C

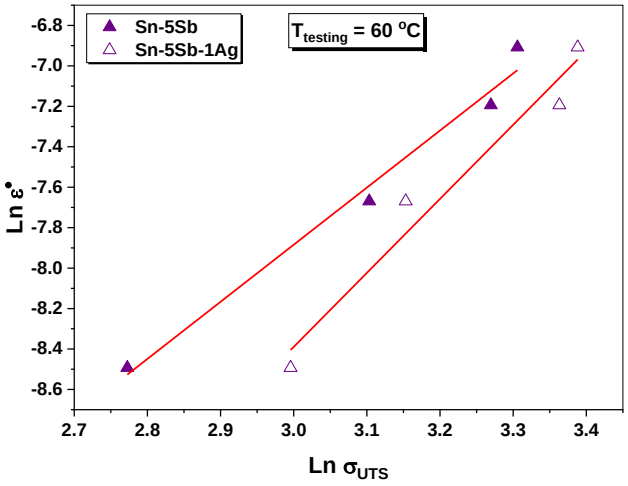

Figure 9: The relation between ln σ_{UTS} and ln ε• for two samples at temperatures 60 °C

The strengthening effect of Sn-based alloys is more noticeable when the value of (n) is larger. Figure 11 illustrates how the values of (n) improved as Ag was added. The development of the recently formed Ag_3Sn IMC and the β-phase refinements may be connected to the resistance to dislocation climb. As shown in Fig. 11, a reduction in n values at higher temperatures may be explained by the greater mobility of current dislocations. The intermetallic compounds act as pinning agents, but thermal energy aids the dislocations in overcoming them [S.W. Chen, 2008].

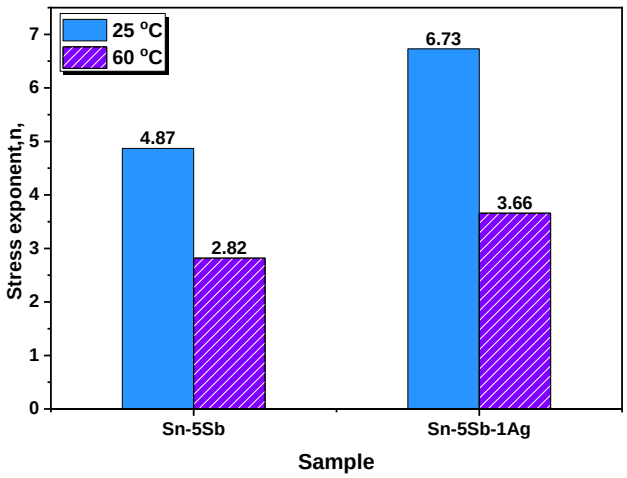

Figure 11: The relationship between n and temperature of two alloys.

4. Conclusion

The influence of adding Ag to Sn-5Sb alloy was the main focus of this investigation. Several conclusions can be made:

1. The binary alloy (Sn-5Sb) has a microstructure consisting of the β-Sn matrix and SbSn phase, which are distinguished by spherical white particles at the grain boundaries.
2. A long rod-shaped Ag_3Sn IMC formed along grain boundaries as a result of the addition of 1 weight percent Ag.
3. Adding 1 weight percent of Ag reduces the average β-Sn particle size.
4. Tensile findings showed that σ_Y and σ_{UTS} increased with the addition of Ag element and increased strain rates.
5. For all investigated samples, the σ_{UTS} and σ_Y decrease when the deformation temperature is raised from 25 to 60 °C.
6. Compared to Sn-5Sb alloy, Sn-5Sb-1Ag has higher stress exponent (n) values.

Acknowledgement

We would like to thank the graduation project supervisor, Dr. Maha Mahmoud, for her guidance and assistance with this research. We also like to thank the head of the physics department and all of the physics department members for their support.

References and Sources

- M. Abtew, G. Selvaduray 95–141 (2000). Lead-free solders in microelectronics. Mater. Sci. Eng.
- E.A. Eid, A.M. Deghady, A.N. Fouda 726–723 (2019). Enhanced microstructural, thermal and tensile characteristics of heat treated Sn-5.0Sb-0.3Cu (SSC-503) Pb-free solder alloy under high pressure. Mater. Sci. Eng.
- Edmond Chan, Stanedy Yue (2004). Lead-Free Soldering in Electronics Manufacturing: A Global Perspective. IEEE Green Electronics Conference
- Morozumi, H. Hokazono, Y. Nishimura, E. Mochizuki, Y. Takahashi 8–17 (2015). Influence of antimony on reliability of solder joints using Sn-Sb binary alloy for

power semiconductor modules. Trans. Jpn. Inst. Electron. Packag.

- Park, OH, 2004 Alloy Phase Diagrams. "ASM Handbook.
- "The phase diagram of tin-antimony system source: Zu et al (2006)"

- Y. Swilem, A. A. El-Daly, Ahmed Hammad (2009). Creep Properties of Sn–Sb Based Lead-Free Solder Alloys. Journal of Alloys and Compounds

- Kyosuke Kobayashia, Ikuo Shohjia, Shinji Koyamaa, Hiroaki Hokazono 238 – 245 (2017) Fracture Behaviours of Miniature Size Specimens of Sn-5Sb Lead Free Solder under Tensile and Fatigue conditions. Procedia Engineering.

- M. M. Mousa, A. F. Abd-ElRehim,and shereen. M.Abdlaziz (2024)- Title: Influence of Cr inclusion on microstructure evolution and tensil properties of Sn-5 wt% Sb solder alloy., J. Electron. Mater.

- Tianhan Hu, Shun Li, Zhen Li, Guanzhi Wu, Ping Zhu, Wufeng Dong, Yu Sun , Ji ayi Zhou , Bingjia Wu , Bingge Zhao , Kai Ding , Yulai Gao, 2023, Coupled effect of Ag and In addition on the microstructure and mechanical properties of Sn–Bi lead-free solder alloy, Journal of Materials Research and Technology.

- S.W. Chen, C.C. Chen, W. Gierlotka, A.R. Zi, P.Y. Chen, H.J. Wu 37, 992–1002 (2008). Phase equilibria of the Sn-Sb binary system, J. Electron. Mater.

- T. Kobayashi, I. Shohji, Y. Nakata, Effect of power cycling and heat aging on reliability and IMC growth of Sn-5Sb and Sn-10Sb solder joints, Advances in Mater. Sci. Eng. 208, 4829508 (2018).

- A.R. Geranmayeh, R. Mahmudi, Power law indentation creep of Sn-5% Sb solder alloy, J. Mater. Sci. 40, 3361–3366 (2005).

- J.H. Kim, S.W. Jeong, H.M. Lee, Thermodynamics-aided alloy design and evaluation of Pb free solders for high-temperature applications, Mater. Trans. 43, 1873–1878 (2002).

- A.Sadeghi, E. Kozeschnik, Modeling the evolution of the dislocation density and yield stress of al over a wide range of temperatures and strain rates, Metallurgical and Materials Transactions A, 55(5), 1643–1653, (2024).

- M.M. Mousa , M.A. Mahmoud, M.M. El-Zhery, M. Sobh, 98, 035712 (2023) . Synergetic role of Ni and GOns to improve the microstructure and mechanical creep

rate of Sn-5.0Sb-0.7Cu solder alloy, Phys. Scr.

- Sadeghi, and E. Kozeschnik, Modeling the evolution of the dislocation density and yield stress of al over a wide range of temperatures and strain rates, Metallurgical and Materials Transactions A, 55(5), 1643–1653(2024)
- Q.S. Zhu, Z.G. Wang, S.D. Wu, J.K. Shang, Enhanced rate-dependent tensile deformation in equal channel angularly pressed Sn–Ag–Cu alloy, Mater. Sci. Eng. A 502, 153–158 (2009).
- K.C. Cham, G.A. Tong, Strain rate sensitivity of high-strain rate super plastic A 16061/20SiCw composite under uniaxial and equiaxial tension, Mater. Lett. 51, 389–395 (2001).
- S.W. Chen, C.C. Chen, W. Gierlotka, A.R. Zi, P.Y. Chen, H.J. Wu, Phase equilibria of the Sn-Sb binary system, J. Electron. Mater. 37, 992–1002 (2008).